

Electrochemical behavior of a passive film formed on Alloy 600

Dong-Jin Kim, Hyuk Chul Kwon, Seong Sik Hwang and Hong Pyo Kim

*Division of Nuclear Material Technology Developments, Korea Atomic Energy Research Institute(KAERI), Yuseong,
Daejeon, Korea, 305-600*

1. Introduction

Alloy 600 is an austenitic Ni-Fe-Cr alloy commonly used as the tubing material in the steam generator of pressurized water reactors(PWR). In a PWR, a steam generator tubing forms the pressure boundary between the primary coolant water that extracts the heat from the nuclear reactor and the secondary water that produces the steam for a power generation. Therefore it is very important to maintain a tube's integrity. In spite of the excellent corrosion resistance of Alloy 600, a lot of stress corrosion cracks have been observed during the operation of nuclear power plants for a long time [1,2].

It is undoubtable that a stress corrosion cracking(SCC) is deeply related to an oxide formed on an Alloy 600 surface while a mechanism to describe a SCC occurrence is still debatable [3-5]. The slip dissolution/film rupture mechanism states that the crack tip is advanced as the protective film is ruptured by increasing the strain in the underlying matrix and that the crack tip is dissolved/repassivated again [3]. According to the internal oxidation mechanism, a SCC of Alloy 600 is based on a diffusion of oxygen into the metal lattice. A brittle cracking can be caused by the presence of a layer of oxygen atoms at the grain boundary, by the formation of an internal oxide or by the formation of a gas bubble [5].

An understanding of the basic electrochemical behaviors regarding an anodic dissolution and a passivation of the bare surface of metals and alloys provides important information about a SCC. Therefore the passive properties of Alloy 600 which is widely used in the nuclear industry should be studied thoroughly.

Under these circumstances, in the present work, the passive oxide films on Alloy 600 were investigated by using a potentiodynamic polarization, an electrochemical impedance spectroscopy(EIS), a depth profiling by an Auger electron spectroscopy(AES) and a transmission electron microscopy(TEM).

2. Experimental

Alloy 600 of a 1cm × 1cm area as a working electrode was mechanically ground with silicon carbide paper up to #2400 followed by an Al₂O₃ polishing and an ultra sonic treatment. A platinum wire and an external Ag/AgCl electrode were used as a counter and a reference electrode, respectively.

Aqueous 0.5M H₃BO₃(pH 4.4), 0.5M Na₂SO₄(pH 6.5), 0.1M NaOH(pH 13.4) and NH₄OH(pH 9.7) solutions as electrolytes were prepared. Deaerated solution was prepared by an N₂ purging for 20hrs.

Potentiodynamic experiment was performed in the potential range from -0.2V(Ag/AgCl) under the open circuit potential(OCP) to 1.5V(Ag/AgCl) with a scan rate of 0.5mV/s. Ac-impedance measurement was carried out in the frequency range of 10⁶ to 10⁻¹ Hz at OCP with a 10mV amplitude perturbation. An ac-impedance measurement was carried out with a Solartron 1255 frequency response analyzer connected to a Solartron 1287 electrochemical interface.

In order to identify the composition and depth of the passive film, AES was used. Sputtering rate was determined to be 138 Å/min with reference to the SiO₂ layer and the oxide thickness used in this work was regarded as the SiO₂ thickness.

Microstructure of the passive film was observed by using TEM(TECNAI, G² F30) whose sample was prepared by use of a field ion beam(FIB).

3. Results and discussion

Fig. 1 shows the Nyquist plots obtained from Alloy 600 at OCP in a deaerated NH₄OH solution at 315°C as a function of the immersion time. Two capacitive arcs were shown in the Nyquist plot, implying that the equivalent circuit for this system consisted of a series of two parallel resistance-capacitance circuits. From the shape of this impedance plot, it is assumed that the oxide films are composed of an outer oxide layer with a lower resistance(high frequency arc) and an inner oxide layer with a relatively higher resistance(low frequency arc). Moreover the size of the two capacitive arcs was changed with the immersion time indicating that the oxide thickness and oxide passive state were varied with the time, based on the kinetics and thermodynamics of the oxide film.

Comparing the aerated aqueous solutions with the deaerated aqueous solutions, the passive current and corrosion potential were decreased in the deaerated solution, indicating that the passivity of the surface film is more protective.

Fig. 2 presents the micrograph of the passive film formed on Alloy 600 in the deaerated NH₄OH solution of pH 9.7 at 315°C for 14 days. From the result of Fig. 2, a duplex structure of an oxide film which is composed of a thick/porous outer oxide and a thin/dense inner oxide was observed.

Fig. 3 shows the oxide resistance(left axis) and oxide thickness(right axis) for the oxide film formed in the 0.5M H₃BO₃ aqueous solutions of 300°C with/without dissolved oxygen. Oxide resistance for an oxide film formed in the deaerated solution was larger than that in the aerated solution whereas the oxide thickness for an

oxide film formed in the deaerated solution was smaller than that in the aerated solution. According to the AES result, Fe content for an oxide film formed in the deaerated solution was a little bit larger than that in the aerated solution(not shown here). It is plausible that the porosity of an oxide film and the chemical state of the elements composing an oxide rather than the oxide thickness are more important factors for determining the passivity of an oxide.

4. Conclusion

The duplex structure of the oxide film formed on Alloy 600 was observed. It was found that the oxide films were composed of an outer oxide layer with a lower resistance and an inner oxide layer with a relatively higher resistance.

The resistance of an oxide formed in the aerated solution was smaller than that in the deaerated solution while the oxide film in the aerated solution was thicker than the oxide film in the deaerated solution indicating that the passivity of an oxide depends on the porosity of an oxide film and the chemical state of the elements composing an oxide rather than the oxide thickness.

REFERENCES

- [1] P. M. Scott and P. Combrade: 11th Int. Conf. Environmental Degradation of Materials in Nuclear Systems, p. 29, Stevenson, WA, Aug. 10-14, 2003.
- [2] J. A. Gorman, J. E. Harris: 11th Int. Conf. Environmental Degradation of Materials in Nuclear Systems, p. 362, Stevenson, WA, Aug. 10-14, 2003.
- [3] P. L. Andresen and F. P. Ford, Mater. Sci. Eng.: A103 (1988) 167.
- [4] D. D. Macdonald and M. Urquidi-Macdonald: Corrosion Science Vol. 47 (1991), p. 51.
- [5] P. M. Scott and M. Le Calvar: 6th Int. Symp. on Environmental Degradation of Materials in Nuclear Power Systems, p. 657, San Diego, CA, Aug. 1-5, 1993.

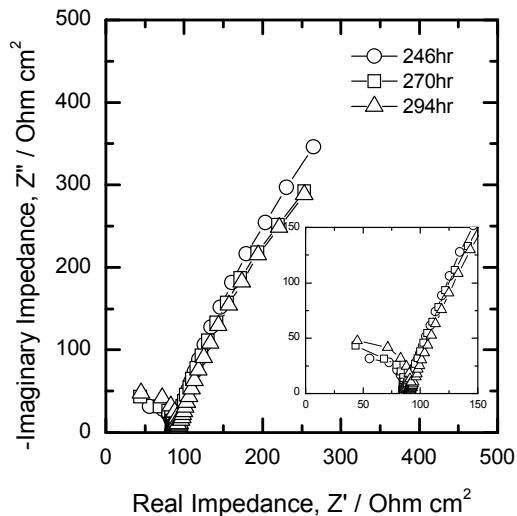
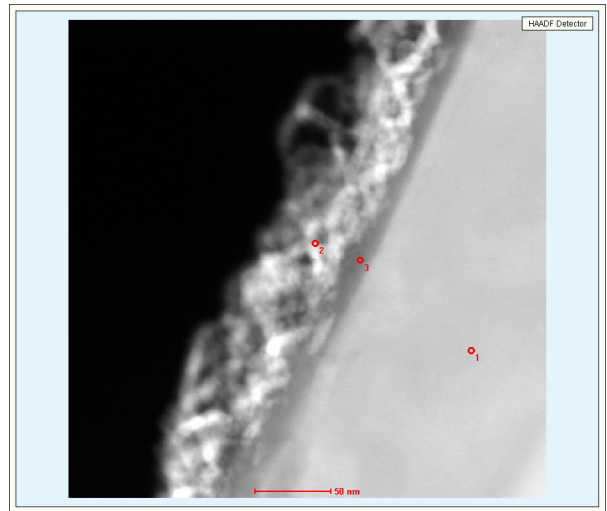


Fig. 1. Nyquist plots obtained from Alloy 600 at OCP in deaerated NH_4OH solution at 315°C .



at%	# 1	◇	# 2	◇	# 3	◇	Remark
Ni	73	73	54	62	49	56	
Fe	11	11	8	9	8	9	
Cr	16	16	25	29	31	35	
O	-		13		12		
	Base metal	No O2	Inner oxide		Outer oxide		~50nm thick

Fig. 2. Micrograph of passive film formed on Alloy 600 in deaerated NH_4OH solution of pH 9.7 at 315°C for 14 days.

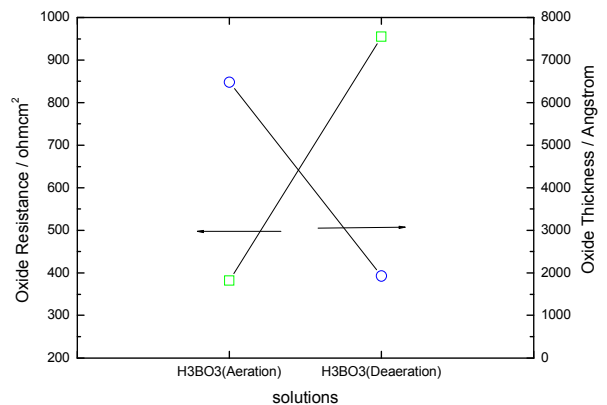


Fig. 3. Oxide resistance(left axis) and oxide thickness(right axis) for the oxide film formed in 0.5M H_3BO_3 aqueous solutions of 300°C with/without dissolved oxygen.